Preparation and Alkali-Metal Ion Extraction/Insertion Reactions with Nanofibrous Manganese Oxide Having 2 × 4 Tunnel Structure

Zong-huai Liu† and Kenta Ooi*

National Institute of Advanced Industrial Science and Technology, 2217-14, Hayashi-cho, Takamatsu, Kagawa, 761-0395 Japan

Received June 19, 2003

Sodium manganese oxide with a 2 × 4 tunnel structure (Na-2 × 4) was hydrothermally synthesized from Na−birnessite material in NaOH solutions at relatively low temperatures. The Na^+ extraction and alkali-metal ion insertion reactions were investigated by chemical and X-ray analyses, SEM observation, FT-IR spectroscopy, TG-DTA analyses, pH titration, and K_d measurements. A considerable amount (81%) of Na^+ ions in the 2 × 4 tunnel sites were topotatically extracted by acid treatment, accompanied by a slight change of the lattice parameters. Alkali-metal ions could be inserted into the 2 × 4 tunnel sites of the acid-treated sample (Na-2 × 4 (H)), mainly by an ion-exchange mechanism. The pH titration study showed that Na-2 × 4 (H) had simple monobasic acid behavior toward alkali-metal ions with a relatively low exchange capacity below pH 10; the exchange capacity increased in the order $Cs^+ < Li^+ < Na^+ < K^+ \cong Rb^+$ at pH 6. The distribution coefficient (K_d) study on Na-2 × 4 (H) showed the selectivity sequence of $Cs^+ < Li^+ < K^+ < Rb^+$ around pH 4. These results suggest that manganese oxide with a 2 × 4 tunnel structure has a weak ion-sieve property for the adsorption of ions with an effective ionic radius around 1.7 Å.

Introduction

Manganese oxides have been intensively investigated during the past few decades because of their economic values and potential applications. They can be used as ion sieves, molecular sieves, catalysts, and cathodic materials in lithium batteries due to their excellent cation-exchange and molecule adsorptive properties as well as their excellent electrochemical and magnetic properties.[1−4] The family of manganese oxides includes layered and one-dimensional tunnel materials, which are composed of corner- or edge-shared MnO_6 octahedral units.[5] Microporous manganese oxides with tunnel structures can be classified into three groups based on the number of MnO_6 octahedral chains between two basal layers.[6] The 1 × *n* group includes pyrolusite (with a 1 × 1 tunnel)[7] and ramsdellite (1 × 2).[8] The 2 × *n* group consists of hollandite (2 × 2),[9] romanechite (2 × 3),[10] and RUB-7 (Rb-2 × 4)[11] and others. Todorokite is a typical representative of the 3 × *n* group.[12]

RUB-type manganese oxides have a one-dimensional (2 × 4) tunnel structure, as shown in Figure 1. Rziha et al.[11] first reported the synthesis of RUB-type manganese oxides with a 2 × 4 tunnel structure, which could be prepared by hydrothermal treatment of alkali−birnessite in hydroxide solutions at 350 °C and 2 kbar for 48 h using a gold capsule. A structural model for the Rb-end member of this family of materials was developed and subsequently refined using the Rietveld technique. The Rb-(2 × 4) tunnel structure has a monoclinic space group and two Rb^+ and one water of crystallization may occupy a unit tunnel. However, chemical analyses and further characterization of RUB-7-type manganese oxide could not be carried out because only small amounts of samples were available. By the hydrothermal soft chemical process, Feng et al.[13] synthesized Na-(2 × 4) tunnel manganese oxide under a relative temperature range from 200 to 300 °C and a concentration range of NaOH solution from 0.5 to 1.0 M. But the synthesized material showed low crystallinity, and only the main diffraction peaks could be confirmed on the X-ray diffraction pattern. Recently, Xia and colleagues[14] developed a new approach for synthesizing Na-2 × 4 tunnel at low temperatures and low pressures by a hydrothermal method; some structural properties for this material have also been studied. The elemental analysis showed that the synthesized mater-

* To whom correspondence should be addressed. Tel: +81-869-3511. Fax: +81-869-3551. E-mail: k-ooi@aist.go.jp.
† E-mail: zonghuai-liu@aist.go.jp.

(1) Shen, Y. F.; Zerger, R. P.; DeGuzman, R. N.; Suib, S. L.; McCurdy, L.; Potter, D. I.; O'Young, C. L. *Science* **1993**, *260*, 511.
(2) Cao, H.; Suib, S. L. *J. Am. Chem. Soc.* **1994**, *116*, 5334.
(3) Feng, Q.; Kanoh, H.; Ooi, K. *J. Mater. Chem.* **1999**, *9*, 319.
(4) Armstrong, A. R.; Huang, H.; Jennings, R. A.; Bruce, P. G. *J. Mater. Chem.* **1998**, *8*, 255.
(5) Burns, R. G.; Burns, V. M. *Manganese Dioxide Symposium*, Tokyo, 1980; Vol. 2, p 97.
(6) Turner, S.; Buseck, P. R. *Science* **1981**, *212*, 1024.
(7) Baur, W. H. *Acta Crystallogr.* **1976**, *B32*, 2200.
(8) Byström, A. M. *Acta Chem. Scand.* **1949**, *3*, 163.
(9) Byström, A.; Byström, A. M. *Acta Crystallogr.* **1950**, *3*, 146.
(10) Wadsley, A. D. *Acta Crystallogr.* **1953**, *6*, 433.
(11) Rziha, T.; Gies, H.; Rius, J. *Eur. J. Mineral.* **1996**, *8*, 675.
(12) Burns, R. G.; Burns, V. M.; Stockman, H. W. *Am. Mineral.* **1983**, *68*, 972.
(13) Feng, Q.; Horiuchi, T.; Liu, L.; Yamagisawa, K.; Mitsushi, T. *Chem. Lett.* **2000**, 284.
(14) Xia, G.-G.; Tong, W.; Tolentino, E. N.; Duan, N.-G.; Brock, S. L.; Wang, J.-Y.; Suib, S. L. *Chem. Mater.* **2001**, *13*, 1585.

10.1021/cm030344z CCC: $25.00
Published on Web 08/12/2003

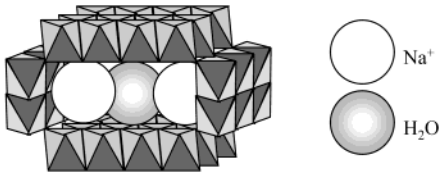

Figure 1. Structure of RUB-7-type manganese oxide with 2 × 4 tunnel structure. The MnO_6 octahedrons link together, sharing edges to form the 2 × 4 tunnel structure.

ial has a formula in one unit cell of $Na_8Mn_{24}O_{48}{\cdot}xH_2O$. The synthetic template materials, the pH value of the medium, and the autoclave temperature were critical for the synthesis. Sodium salts, such as NaCl, $NaNO_3$, or Na_2SO_4, were good templates for Na-2 × 4. In a strong basic solution or below 160 °C, Na−birnessite did not transform to the Na-2 × 4 tunnel structure.

We found that Na−birnessite can also be transformed to a Na-2 × 4 tunnel structure, even in a strong basic solution at a relatively low temperature. The synthesized Na-2 × 4 tunnel manganese oxide is expected to have ion-sieve properties when the metal ions in the tunnel are extracted, similar to other tunnel-type manganese oxides such as hollandite- or todorokite-types. However, because the metal ion adsorptive properties of Na-2 × 4 tunnel manganese oxide have not yet been clarified, this will restrict its application. The present paper reports the conditions for synthesis of Na-2 × 4 tunnel manganese oxide and its metal ion extraction/insertion reactions in aqueous phase.

Experimental Section

Sample Preparation. Na-2 × 4 tunnel manganese oxide was hydrothermally synthesized using Na−birnessite manganese oxide as precursor in 2 M NaOH solution at low temperature (150 °C) and autogenous pressure. The starting material, layered manganese oxide (Na−birnessite), was prepared by the method reported in the literature,[15] as follows. A mixed solution of 0.6 M NaOH and 2 M H_2O_2 was poured quickly into a 0.3 M $Mn(NO_3)_2$ solution and stirred for 25 min. The black precipitate obtained was washed several times with distilled deionized water until the pH reached around 7, which had a chemical formula of $Na_{3.1}Mn_{12}O_{23}{\cdot}8H_2O$.

A wet Na−birnessite sample (4 g in a dried state) and 80 mL of 2 M NaOH solution were sealed in a 100-mL autoclave in a Teflon-lined stainless steel vessel and autoclaved at 150 °C under autogenous pressure for 10 days. The obtained gray-black solids were thoroughly washed with distilled deionized water and then dried at 70 °C for 1 day. Sodium manganese oxide with a 2 × 4 tunnel structure was obtained, which is hereafter abbreviated as Na-2 × 4.

Metal Ion Extraction/Insertion Reactions. In the extraction reaction, Na-2 × 4 (2 g) was immersed in 1, 5, or 10 M nitric acid solutions (200 mL) for 5 days. The acid-treated sample with 10 M HNO_3 solution is hereafter abbreviated as Na-2 × 4 (H). In the insertion reaction, Na-2 × 4 (H) (1 g) was immersed in a 1 M MOH (M = Li, Na, K, Rb, or Cs) solution (100 mL) for 7 days to obtain alkali-metal ion-inserted samples. The inserted samples are hereafter abbreviated as 2 × 4 (M), where M represents the inserted metal ions: (2 × 4 (Li), 2 × 4 (Na), 2 × 4 (K), 2 × 4 (Rb), or 2 × 4 (Cs)). The metal ion-inserted samples were further treated with a 1 M HNO_3 solution for 2 days to investigate the re-extractability of alkali-metal ions. They are abbreviated as 2 × 4 (M−H) for alkali-metal ion M. The extracted and inserted samples were filtered, washed with water, and air-dried at room temperature for 2 days.

pH Titration. Each Na-2 × 4 (H) sample (0.05 g) was immersed in a mixed solution (5 mL) of 0.1 M MCl + MOH (M = Li, Na, K, Rb, and Cs) in varying ratios with intermittent shaking at 25 °C. After the sample was shaken for 7 days, the pH of the supernatant solution was determined with a Horiba Model M-13 pH meter.

Distribution Coefficient (K_d). K_d values of alkali-metal ions were determined by a batch method. A 0.1-g portion of Na-2 × 4 (H) sample was immersed in 10 mL of a solution containing 10^{-3} M each of Li^+, Na^+, K^+, Rb^+, and Cs^+ at different pH values. The pH values were changed using MOH instead of MCl (M = Li, Na, K, Rb, or Cs). After attaining equilibration (7 days), the metal ion concentrations in the solution were determined by atomic absorption spectrometry. The metal ion uptake was calculated from the decrease of concentration relative to the initial concentration in the solution. The K_d value was calculated using the following equation:

$$K_d\,(\mathrm{mL/g}) = \frac{\text{metal ion uptake (mmol/g of sample)}}{\text{metal ion concentration (mmol/mL solution)}}$$

Chemical Analysis. The mean oxidation number (Z_{Mn}) of manganese was evaluated from the value of available oxygen, which was determined by the standard oxalic acid method as described elsewhere.[16] The alkali metal and manganese contents were determined by atomic absorption spectrometry after the samples were dissolved in a mixed solution of HCl and H_2O_2.

Physical Properties. X-ray diffraction (XRD) analysis was carried out using a Rigaku-type RINT 1200 X-ray diffractometer with a graphite monochromator at room temperature. Infrared spectra were obtained by the KBr method on a Perkin-Elmer infrared spectrometer (1600 Series FTIR). TG-DTA curves were obtained on a MAC Science thermal analyzer (system 001, TG-DTA 2000). The experiments were conducted under an air atmosphere (100 mL/min) at a heating rate of 10 °C /min. The water content of the samples was calculated from the weight loss of the TG curve in the temperature range 30−400 °C. SEM observation was carried out with a Hitachi-type S-2460N scanning electron microscope.

Results and Discussion

Preparation of Na-2×4 Manganese Oxide. It has been reported that the synthetic template materials, the pH value of the medium, and the autoclaved temperature are critical in the preparation of Na-2 × 4-type manganese oxide.[11,13,14] In this work, sodium ions were selected as the template material and the transformation from a birnessite layered structure to a tunnel structure was studied in a NaOH solution. The X-ray diffraction patterns of samples obtained in NaOH solutions with different concentrations are shown in Figure 2. Na−birnessite prepared by reacting Mn^{2+} and H_2O_2 in a NaOH solution has a layered structure with a basal spacing of 7.19 Å (Figure 2a). The synthesized Na−birnessite was soaked in NaOH solutions with different concentrations, and the mixtures were sealed in a 100-mL autoclave in a Teflon liner and hydrothermally heated at 150 °C for 10 days with intermittent shaking. The crystal phase of the precipitates after hydrothermal treatment depends on the concentration of the NaOH solution. The layered birnessite structure does not transform into a 2 × 4 tunnel structure in solutions with high NaOH concentration. The layered structure is

(15) Feng, Q.; Sun, E.-H.; Yamagisawa, K.; Yamasaki, N. *J. Ceram. Soc. Jpn.* **1997**, *105*, 564.

(16) Japan Industrial Standard (JIS), 1969, M8233.

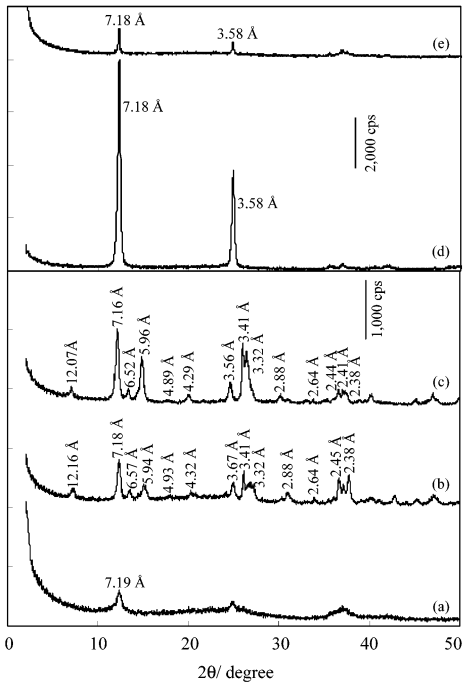

Main peak indexing of Na–2×4

d (Å)	h k l
12.07	0 0 2
7.16	2 0 0
6.52	-2 0 2
5.96	0 0 4
4.89	-2 0 4
4.29	2 0 4
3.56	4 0 0
3.41	-4 0 3
3.32	4 0 2
2.88	4 0 4
2.64	-4 0 7
2.44	-4 0 8
2.41	3 1 1
2.38	6 0 0

Figure 2. XRD patterns of the samples obtained by hydrothermal treatment of the starting Na−birnessite in NaOH solutions of different concentrations: (a) starting Na−birnessite, (b) 1 M, (c) 2 M, (d) 4 M, and (e) 6 M.

maintained and the basal spacing of the layered structure of Na−birnessite does not change at $M_{NaOH} > 2$, although the intensity of the peaks at $d = 7.19$ Å increases due to the hydrothermal treatment (Figure 2d,e). On the other hand, a good crystalline Na-2 × 4 with black nanofiber is yielded when $M_{NaOH} \leq 2$. The first peak appears at a d spacing of 12.07 Å in the [0 0 2] direction. The second peak has a similar d spacing of 7.16 Å in the [2 0 0] direction with Na−birnessite in the [1 0 0] direction (Figure 2b,c), which agrees with the results in the literature.[14] This indicates that the layered birnessite is converted slowly to a 2 × 4 tunnel structure in a NaOH solution below 160 °C in an autoclave. The conditions under which 2 × 4 tunnels form are different from those in the literature,[13,14] that is, that the transformation of Na−birnessite to Na-2 × 4 did not occur when it was heated at 160 °C for 10 days in an autoclave.

The SEM observation shows that the synthesized Na-2 × 4 material consists of nanofibers with a thickness of about 80 nm (Figure 3a). The lattice parameters are $a = 14.4$ Å, $b = 2.84$ Å, $c = 23.9$ Å, and $\beta = 98.0°$, which are close to those values reported by Xia et al. ($a = 14.43$ Å, $b = 2.85$ Å, $c = 23.98$ Å, and $\beta = 98.0°$, respectively.).[14] Compared to the lattice parameters of Rb-2 × 4 ($a = 14.19$ Å, $b = 2.85$ Å, $c = 24.34$ Å, and $\beta = 91.29°$), the a axis of Na-2 × 4 is a little longer while the c axis is a little shorter and the β value larger. The Na-2 × 4 crystal grows along the b direction or the tunnel direction.

Elemental analyses indicate that the synthesized Na-2 × 4 tunnel material has a formula in one unit cell of $Na_8Mn_{27}O_{53}{\cdot}9H_2O$. The average oxidation state of manganese is 3.63, which is a little higher than that of the starting Na−birnessite (3.57).

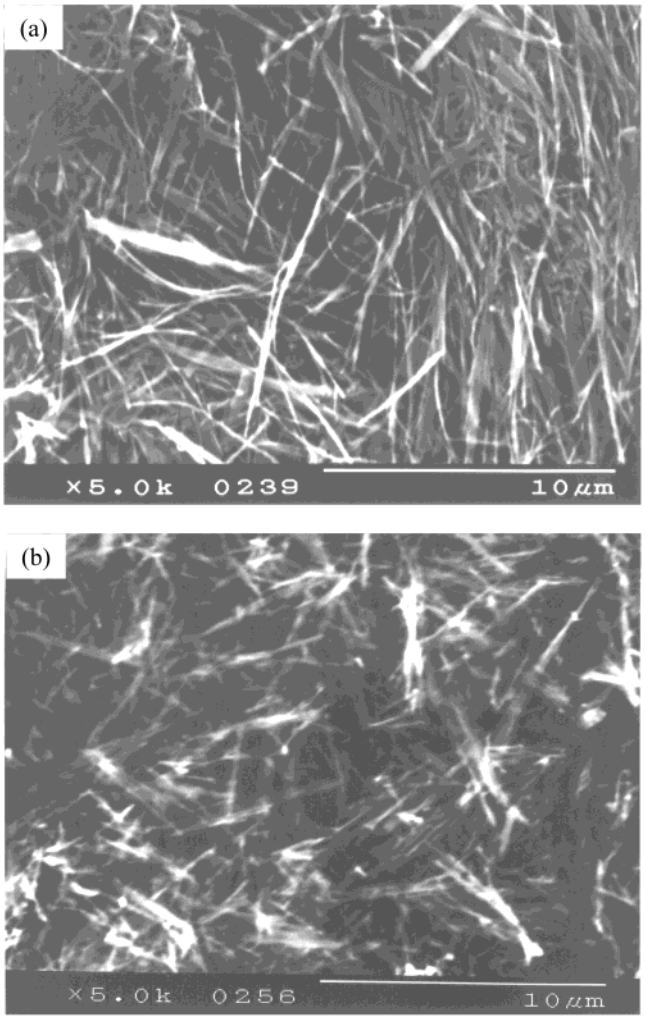

Figure 3. SEM image of (a) Na-2 × 4 and (b) Na-2 × 4 (H).

The layered manganese oxides are easily maintained under strongly basic conditions, while the structural transformations from layered-type to tunnel-type manganese oxides appear to occur more readily in neutral or weakly basic solutions. We analyzed the amount of incorporated Na^+ ions for samples obtained in NaOH solutions with different concentrations and found that the amount increased with an increase in the NaOH concentration. The Na^+ content of samples increased from 2.95 to 3.36 mmol/g with an increase in the NaOH concentration from 1 to 4 M. The transformation from layered to tunnel structure requires the migration of some Mn atoms from manganese oxide sheets to interlayer positions. The densely packed interlayer Na^+ ions may suppress the migration of Mn atoms, inhibiting the transformation from layered to tunnel structure. Usually, the transformation from layered to tunnel structure is accompanied by a slight increase of the mean oxidation number of manganese (Z_{Mn}) and a decrease of water amount.[17,18] A similar tendency is also observed for the present transformation process from layered birnessite to the Na-2 × 4 tunnel manganese oxide.

(17) Brock, S. L.; Duan, N.; Tian, Z.; Giraldo, O.; Zhou, H.; Suib, S. L. *Chem. Mater.* **1998**, *10*, 2619.
(18) Shen, Y. F.; Zerger, R. P.; DeGuzman, R. N.; Suib, S. L.; McCurdy, L.; Potter, D. I.; O'Yong, C. L. *Science* **1993**, *260*, 511.

Table 1. Chemical Analysis of Na-2 × 4 and Its Samples Acid-Treated in HNO_3 Solutions of Different Concentrations

samples	Na content (mmol/g)	Na extraction (%)	Mn content (mmol/g)	Mn dissolved (%)	Z_{Mn}[b]	H_2O content (mmol/g)
Na-2 × 4	2.95	N.D.[a]	10.1	N.D.[a]	3.63	3.01
acid-treated (1 M)	1.13	61.7	10.8	9.4	3.78	3.36
acid-treated (5 M)	0.82	72.2	10.9	11.1	3.84	3.48
Na-2 × 4 (H)	0.56	81.1	10.8	11.3	3.85	3.52

[a] N.D.: not determined. [b] Z_{Mn}: mean oxidation number of manganese.

Acid Treatment of Na-2×4. Samples of Na-2 × 4 were soaked in 1, 5, or 10 M HNO_3 solutions, respectively, at room temperature for 5 days. The acid treatment results in the extraction of the Na^+ ions from the tunnel sites, the extractability of the Na^+ ions increases with an increase in the HNO_3 concentrations, and 62, 72, and 81% of the Na^+ ions are extracted at HNO_3 concentrations of 1, 5, and 10 M, respectively. Small amounts of Mn are dissolved in the solutions by the acid treatment (9, 11, and 11%, respectively) (Table 1). The XRD analyses of the acid-treated samples (Na-2 × 4 (H)) show that the main peaks for the 2 × 4 tunnel structure are maintained, although the peak (3.32 Å) corresponding to the [4 0 2] direction weakens gradually while the peak (2.41 Å) corresponding to the [3 1 1] direction strengthens. In addition, the peaks (6.52 and 4.29 Å) in the [−2 0 2] and [2 0 4] directions shift a little with the increase of HNO_3 concentration (Figure 4). The lattice parameters decreased slightly to a = 14.1 Å, b = 2.82 Å, c = 23.2 Å, and β = 95.9° by the acid treatment; the degrees of decrease are marked for a and c values (Table 2). Since the a and c axes are perpendicular to the b axis, which is parallel to the direction of the 2 × 4 tunnel, the Na^+ extraction results in a large shrinkage of the lattice perpendicular to the 2 × 4 tunnel. A SEM image of the acid-treated sample does not show any obvious change in the particle morphology of the nanofibrous form; the particle size merely seems to become smaller (Figure 3b). These results indicate that the extraction reaction progresses topotactically, maintaining the 2 × 4 tunnel structure.

The acid-treated sample (Na-2 × 4 (H)) had a formula of $Na_{1.4}H_{4.6}Mn_{27}O_{55}\cdot 6H_2O$. The amount of protons in the exchange sites could be evaluated from the weight loss in the TG-DTA curve between 160 and 240 °C, similar to the case of spinel-type manganese oxide (Figure 5b).[19] The mean oxidation number (Z_{Mn}) of manganese increases from 3.63 to 3.85 by the acid treatment, owing to a disproportionation reaction of Mn(III) to Mn(IV) and Mn(II) in the acid solution and the dissolution of Mn^{2+} from the tunnel sites.[20−22] Similar behaviors are also observed during the extraction of alkali-metal ions from spinel-type and hollandite-type manganese oxides, where the disproportionation of Mn(III) progresses by a redox-type extraction reaction.[23−25] The smaller cation content, compared to the starting Na-2 × 4 sample, may be caused by the increase in the oxidation number of manganese, which decreases the amount of charge-compensating interlayer cations.

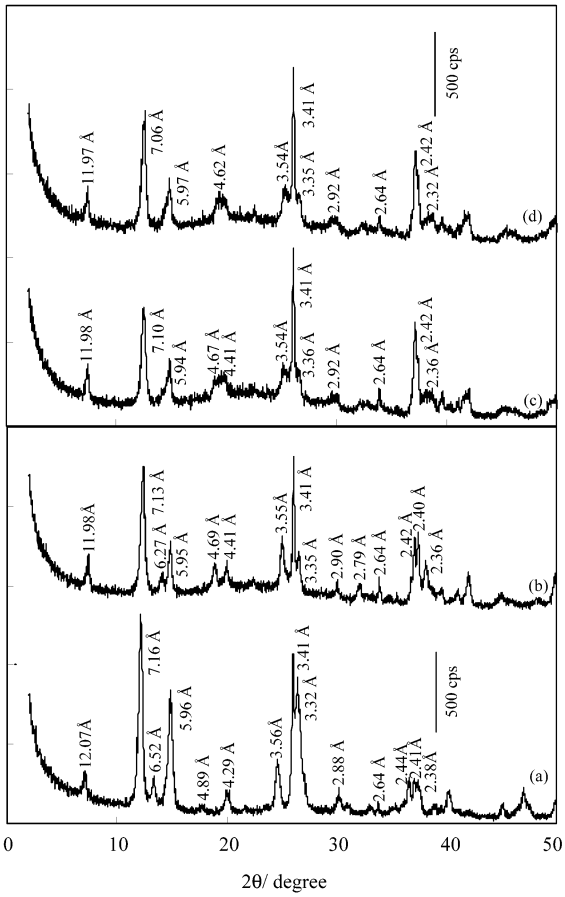

Figure 4. XRD patterns of Na-2 × 4 and its acid-treated samples: (a) Na-2 × 4, (b) in 1 M HNO_3, (c) in 5 M HNO_3, and (d) in 10 M HNO_3.

Table 2. Lattice Parameters of Starting, Acid-Treated, and Reinserted Samples

samples	lattice parameters			
	a (Å)	b (Å)	c (Å)	β
Na-2 × 4	14.4	2.84	23.9	98.0°
acid-treated (1 M HNO_3)	14.2	2.82	23.7	93.4°
acid-treated (5 M HNO_3)	14.2	2.82	23.6	93.9°
Na-2 × 4 (H) (10 M HNO_3)	14.1	2.82	23.2	95.9°
2 × 4 (Li)	14.2	2.82	23.6	96.0°
2 × 4 (Na)	14.5	2.83	24.1	98.5°
2 × 4 (K)	14.3	2.82	24.3	95.9°
2 × 4 (Rb)	14.3	2.82	24.3	95.5°
2 × 4 (Cs)	14.3	2.82	24.2	95.1°

Physical Properties of Na-2×4 and Na-2×4 (H). The TG-DTA curve for the Na-2 × 4 sample shows an endothermic peak around 134 °C (Figure 5a) due to the evaporation of the crystal waters. The endothermic peak at 597 °C with a weight loss can be ascribed to the transformation of Mn(IV) to Mn(III) with the release of oxygen.[20] The Na-2 × 4 (H) sample shows two additional peaks at 227 °C endothermic and 349 °C exothermic in addition to the endothermic peaks at 150 and 597 °C (Figure 5b). The endothermic peak at 227 °C ac-

(19) Feng, Q.; Miyai, Y.; Kanoh, H.; Ooi, K. *Chem. Mater.* **1993**, *5*, 311.
(20) Feng, Q.; Miyai, Y.; Kanoh, H.; Ooi, K. *Langmuir* **1992**, *8*, 1861.
(21) Tsuji, M.; Komarneni, S. *J. Mater. Res.* **1993**, *8*, 611.
(22) Hunter, J. C. *J. Solid State Chem.* **1981**, *39*, 142.
(23) Ooi, K.; Miyai, Y.; Sakakihara, J. *Langmuir* **1991**, *7*, 1167.
(24) Feng, Q.; Kanoh, H.; Miyai, Y.; Ooi, K. *Chem. Mater.* **1995**, *7*, 148.
(25) Ooi, K.; Miyai, Y.; Katoh, S.; Maeda, H.; Abe, M. *Langmuir* **1989**, *5*, 150.

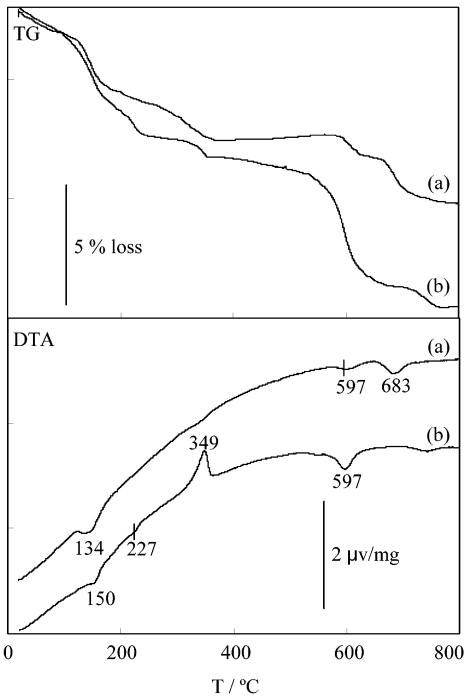

Figure 5. TG-DTA curves of (a) Na-2 × 4 and (b) Na-2 × 4 (H).

companies the weight loss and is ascribed to the dissipation of water by condensation of the lattice −OH groups that are formed by the Na^+/H^+ ion-exchange reaction. The weight loss (1.77%) between 160 and 250 °C corresponds to the proton content of 1.96 mmol/g, which is close to the exchanged Na^+ content (2.39 mmol/g) of the initial Na-2 × 4 sample. The exothermic peak at 349 °C can be ascribed to the transformation from a 2 × 4 tunnel to amorphous phase since the sample heat-treated at 350 °C showed an amorphous structure. The slight weight loss (0.9%) indicates the dissipation of some compounds from the solid during the transformation, but we could not determine the chemical species of the dissipated materials.

IR spectra of Na-2 × 4 and Na-2 × 4 (H) are shown in Figure 6. In the spectrum for Na-2 × 4 (Figure 6a), the bands at 3436 and 3530 cm^{-1} can be assigned to the stretching vibrations of the −OH group of adsorbed water and crystal water molecules, respectively. The former corresponds to the position of the vibration of hydrogen-bonded water and the latter to that of rather isolated water.[26] The band at 1630 cm^{-1} corresponds to the bending vibration of the −OH group. Bands in the region between 400 and 800 cm^{-1} (438, 504, 556, and 744 cm^{-1}) can be assigned to Mn−O lattice vibrations.[5,19,27−29] Similar bands are also observed in hollandite-type or todorokite-type manganese oxides with tunnel structures.[30,31] The bands at 1149 and 1085 cm^{-1} can be assigned to the vibration of the Mn^{3+}−O bond,

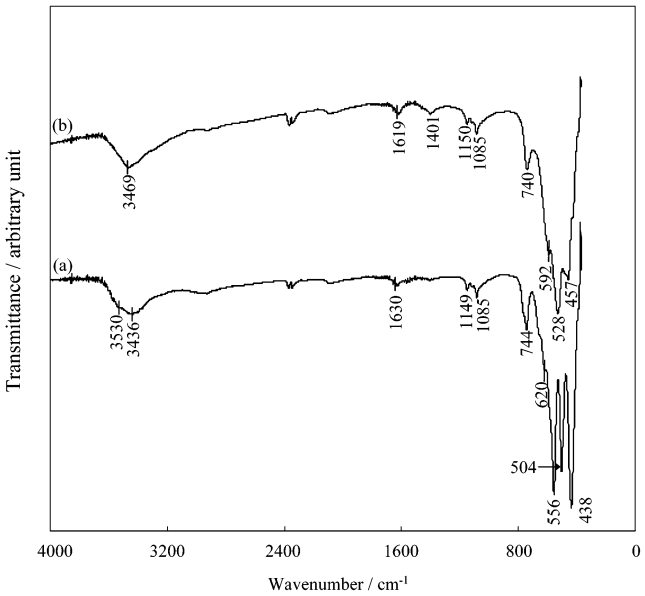

Figure 6. IR spectra of (a) Na-2 × 4 and (b) Na-2 × 4 (H).

as is shown in the literature.[28,32] This suggests the presence of the Mn^{3+} in the crystal of the tunnel structure. In the IR spectrum of Na-2 × 4 (H) (Figure 6b), a remarkable change in the Mn−O stretching region can be observed, although the lattice vibration bands based on the 2 × 4 tunnel structure remain between 400 and 800 cm^{-1}. The four vibration bands become three; the intensities of the bands at 438 and 556 cm^{-1} weaken and their positions shift a little compared to the spectrum of Na-2 × 4. The variations in local structure between the two samples are probably to the difference in the fraction of Mn vacancies or the Mn^{3+} contents.[33] The bands at 3469 and 1619 cm^{-1} can be assigned to stretching and bending vibrations of the −OH group, respectively. The absence of the band around 3530 cm^{-1} suggests that the crystal water interacts strongly with the cations in the tunnel. An unidentified peak is observed at 1401 cm^{-1} for the acid-treated sample.

Insertion of Alkali-Metal Ions. The X-ray diffraction patterns of the alkali-metal ion-inserted samples (2 × 4 (Li), 2 × 4 (Na), 2 × 4 (K), 2 × 4 (Rb), and 2 × 4 (Cs) show that the 2 × 4 tunnel structure remains after the insertion (Figure 7). The alkali-metal ion insertions to Na-2 × 4 (H) result in a slight increase in the lattice constants (Table 2). The sodium-inserted sample has lattice parameters similar to those in the starting Na-2 × 4. These results indicate that the reinsertion reaction also progresses topotactically, maintaining the 2 × 4 tunnel structure.

The chemical compositions of the alkali-metal ion-inserted samples are given in Table 3. The inserted amount of alkali-metal ions decreases in the order $Na^+ > K^+ \approx Li^+ > Rb^+ > Cs^+$. The order agrees with the increasing order of ionic radius of alkali-metal ions, except for Li^+ ions. This suggests that the insertion reaction is subject to the steric effect dictated by the size of the 2 × 4 tunnel. The relatively small amount of

(26) Nyguist, R. A.; Kagel, R. O. *Infrared Spectra of Inorganic Compounds*; Academic Press: New York, 1971; p 3.
(27) Shen, X. M.; Clearfield, A. *J. Solid State Chem.* **1986**, *64*, 270.
(28) Yang, D. S.; Wang, M. K. *Chem. Mater.* **2001**, *13*, 2589.
(29) Feng, Q.; Kanoh, H.; Miyai, Y.; Ooi, K. *Chem. Mater.* **1995**, *7*, 1722.
(30) Golden, D. C.; Chen, C. C.; Dixon, J. B. *Clays Clay Miner.* **1987**, *35* (4), 271.
(31) Golden, D. C.; Chen, C. C.; Dixon, J. B. *Science* **1986**, *231*, 717.
(32) Potter, R. M.; Rossman, G. R. *Am. Mineral.* **1979**, *64*, 1199.
(33) Aronson, B. J.; Kinser, A. K.; Passerini, S.; Smyrl, W. H.; Stein, A. *Chem. Mater.* **1999**, *11*, 949.

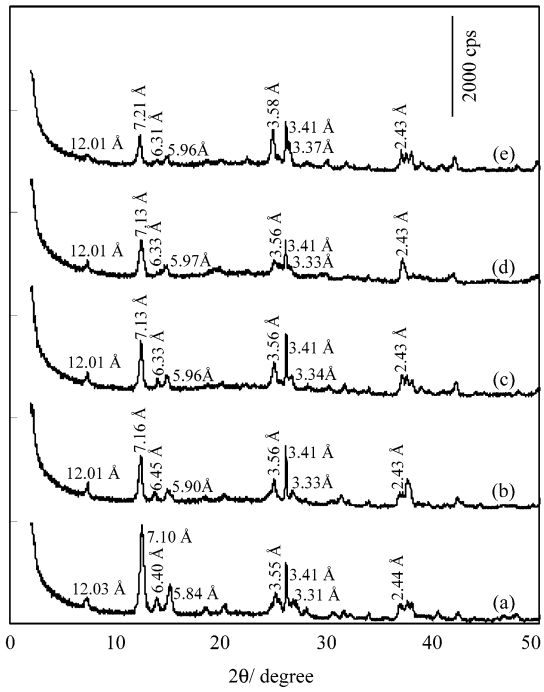

Figure 7. XRD patterns of alkali-metal ion-inserted samples: (a) Li^+-inserted, (b) Na^+-inserted, (c) K^+-inserted, (d) Rb^+-inserted, and (e) Cs^+-inserted.

Table 3. Compositional Analyses of Alkali-Metal Ion-Inserted Samples

sample	M[a] ion content (mmol/g)	Mn content (mmol/g)	M[a]/Mn	Z_{Mn}[b]	H_2O content (mmol/g)
2 × 4(Li)	1.56	10.7	0.15	3.73	2.33
2 × 4(Na)	2.14	10.5	0.21	3.77	2.68
2 × 4(K)	1.56	10.5	0.15	3.80	2.46
2 × 4(Rb)	0.83	10.4	0.08	3.83	2.64
2 × 4(Cs)	0.64	9.94	0.06	3.85	3.29

[a] M = Li^+, Na^+, K^+, Rb^+, or Cs^+. [b] Z_{Mn}: mean oxidation number of manganese.

Li^+ loading suggests that Li^+ ions are inserted into the tunnel in a partially hydrated form. The Na^+/Mn ratio for 2 × 4 (Na) reaches 90% of the initial Na-2 × 4, indicating that the extraction/insertion reaction progresses smoothly. The crystal water content decreases with the insertion of the alkali-metal ions due to the ion exchange of some lattice −OH groups as well as the exclusion of water molecules.

The insertion reactions cause a decrease of the Z_{Mn} value for 2 × 4 (Li) and 2 × 4 (Na) samples. In addition, small amounts of O_2 evolve by the insertion of Li^+ and Na^+ and the color of the supernatant solutions becomes slightly greenish due to the formation of Mn(VI). This indicates that a redox-type insertion reaction occurs, in addition to the Li^+/H^+ and Na^+/H^+ ion-exchange reactions. The redox-type insertion reaction necessitates a reduction of Mn(IV) to Mn(III) as well as an oxidation of OH^- (or H_2O) to oxygen gas. It also accompanies a disproportionation reaction of Mn(IV) to Mn(III) and Mn(VII) or Mn(VI) at the solid surface.[34] Redox-type insertion reactions have also been observed in the cases of alkali-metal ion insertions to spinel-, hollandite-, todorokite-, and birnessite-type manganese oxides.[23,24,29,35] Usually, the supernatant solutions become purple with the formation of Mn(VII) ions. The formation of greenish Mn(VI) has been observed for the Li^+ insertion to the spinel-type manganese oxide derived from Mg_2MnO_4 only.[36] The Z_{Mn} value hardly changes in the case of K^+, Rb^+, and Cs^+ insertions and the coloring by Mn(VI) is not observed. These results suggest that only the ion-exchange reaction proceeds during the insertions of K^+, Rb^+, and Cs^+ ions into Na-2 × 4.

Table 4. Compositional Analyses after 1 M HNO_3 Treatment for Alkali-metal Ion Inserted Samples

sample	M[a] re-extractability (%)	Mn content (mmol/g)
2 × 4(Li−H)	90	10.9
2 × 4(Na−H)	50	10.6
2 × 4(K−H)	34	10.7
2 × 4(Rb−H)	23	10.2
2 × 4(Cs−H)	19	9.98

[a] M = Li^+, Na^+, K^+, Rb^+, or Cs^+.

Re-extraction reactions of alkali-metal ions were investigated using a 1 M HNO_3 solution for the alkali-metal ion-inserted samples. The re-extractability of alkali-metal ions is 90, 50, 34, 23, and 19% for Li^+-, Na^+-, K^+-, Rb^+-, and Cs^+-inserted samples, respectively (Table 4). This suggests that Li^+ ions with a small ionic radius can migrate easily in the (2 × 4) tunnel, but the metal ions (K^+, Rb^+, and Cs^+) with large ionic radii are fixed tightly on the (2 × 4) tunnel sites. The X-ray diffraction patterns of the acid-treated samples show that the re-extraction of the alkali-metal ions also progresses topotactically.

TG-DTA analyses were carried out for the alkali-metal ion-inserted samples (Figure 8). TG-DTA curves of 2 × 4 (Na) are similar to those of the initial Na-2 × 4 sample due to the insertion of Na^+ ions up to of 90% of the exchanged site. Endothermic peaks around 197, 282, and 611 °C, each with a weight loss, are observed. The former two peaks are caused by the dissipation of the crystal water molecules and the latter by the transformation of Mn(IV) to Mn(III) with the release of oxygen (Figure 9b). For the 2 × 4 (K) sample, since the lattice protons in the 2 × 4 tunnel sites are almost all exchanged for K^+ ions, the weight loss by heating to 400 °C is the smallest among the alkali-metal ion-inserted samples. The endothermic peak around 600 °C is the highest for the K^+-inserted sample, probably due to the fact that the inserted K^+ ions are fixed in the 2 × 4 tunnel sites as a pillaring agent (Figure 9c). The Cs^+-inserted sample shows endothermic peaks at 155 and 225 °C with weight losses, due to a considerable amount of lattice protons remaining; the TG-DTA curves are similar to those of Na-2 × 4 (H) (Figure 9d).

pH Titration. The pH titration curves of Na-2 × 4 (H) in (0.1 M MCl + MOH, M = Li, Na, K, Rb, and Cs) solutions are given in Figure 9. All the titration curves show apparently simple monobasic acid behaviors toward alkali-metal ions, similar to those of hollandite-type manganese oxides,[24] but different from those of todorokite-type manganese oxides where the titration

(34) Kanzaki, Y.; Taniguchi, A.; Abe, M. *J. Electrochem. Soc.* **1991**, *138*, 333.

(35) Feng, Q.; Kanoh, H.; Miyai, Y.; Ooi, K. *Chem. Mater.* **1995**, *7*, 1226.

(36) Miyai, Y.; Ooi, K.; Katoh, S. *J. Colloid Interface Sci.* **1989**, *130* (2), 535.

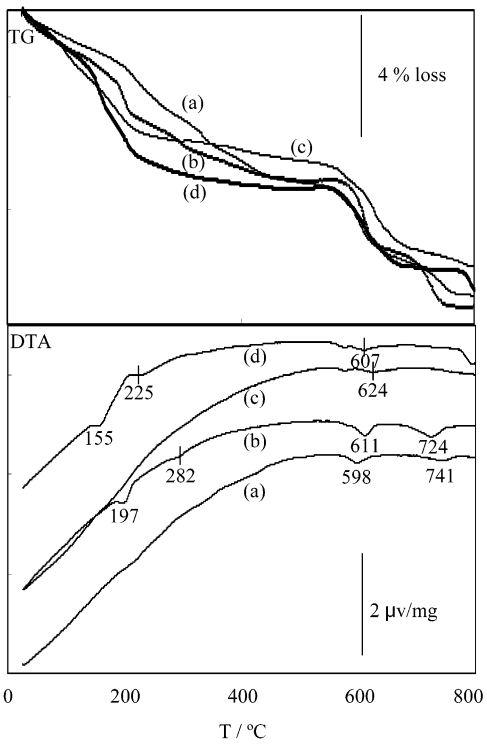

Figure 8. TG-DTA curves of alkali-metal ion-inserted samples: (a) Li^+-inserted, (b) Na^+-inserted, (c) K^+-inserted, and (d) Cs^+-inserted.

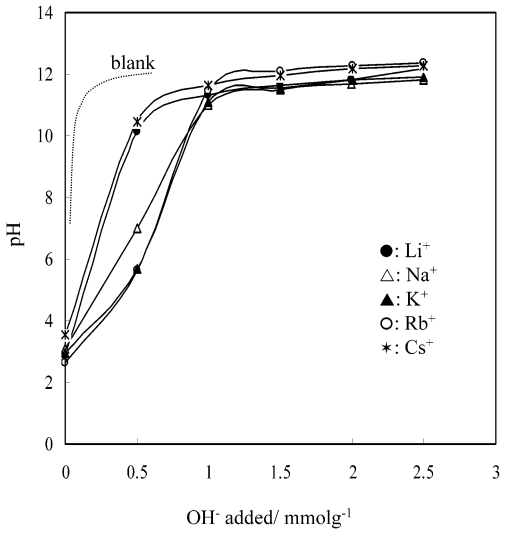

Figure 9. pH titration curves for Na-2 × 4 (H): sample, 0.1 g; solution, 0.1 M MCl + MOH (M = Li^+ (●), Na^+ (△), K^+ (▲), Rb^+ (○), or Cs (*)); total volume of solution, 10 mL; temperature, 25 °C; (·····) blank titration.

curves show multi-basic acid behaviors.[29] The apparent ion-exchange capacity can be evaluated from the amount of OH^- consumed at a known pH, assuming an ion-exchange reaction. The capacity at pH 6 increases in the order Cs ≅ Li < Na < K ≅ Rb, indicating potassium and rubidium ion-sieve properties. The affinity order is different from those of hollandite-type or todorokite-type manganese oxides (Cs < Na < K < Li and Cs < Na ≅ K < Li, respectively). The ion-exchange capacities (0.5, 0.9, 1.0, 1.0, and 0.5 mmol/g for Li^+, Na^+, K^+, Rb^+, and Cs^+, respectively) of Na-2 × 4 (H) are markedly smaller than the corresponding metal ion uptakes (1.56, 2.14, 1.56, 0.83, and 0.64 mmol/g, respectively) in 0.1 M MOH

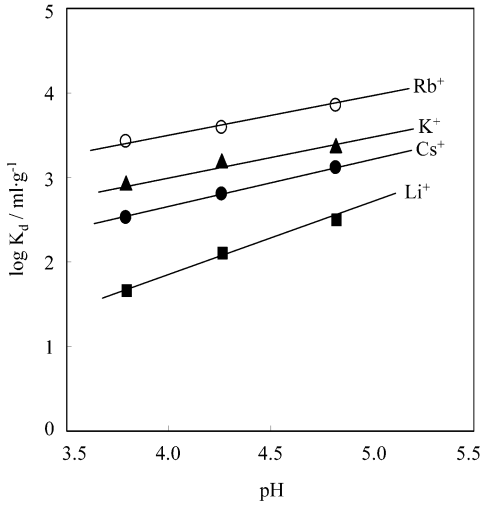

Figure 10. Plots of the distribution coefficients (K_d) of alkali-metal ions on the Na-2 × 4 (H) vs solution pH.

solutions described in Table 3. This suggests that Na-2 × 4 (H) has two kinds of adsorption sites: one is a moderately acidic site exchangeable below pH 10 and the other a very weak acidic site only exchangeable in a strong basic solution. The presence of two kinds of sites can be assumed from the structural characteristics of Na-2 × 4 in which two metal ions and one water can occupy a unit tunnel.

Selectivity of Alkali-Metal Ions. We can evaluate the intrinsic affinity between ion-exchange sites and guest ions from the K_d measurement. Since the K_d value is evaluated under the condition of markedly low metal ion loading, we can ignore the steric interactions between the inserted metal ions. On the other hand, in the pH titration study, the influence of steric interaction strengthens at a higher loading of metal ions, and so it does not reflect exactly the intrinsic affinity between the exchange site and metal ions, but partly reflects the steric interaction between the loaded metal ions. The pH titration is rather suitable for studying the overall exchange behaviors from a microamount to macroamount of loading. From this standpoint, we think that the K_d measurement is suitable for evaluating the ion-sieve property of an inorganic ion exchanger. The equilibrium K_d values of alkali-metal ions on Na-2 × 4 (H) are plotted as a function of solution pH in Figure 10. The K_d values of Na^+ could not be determined accurately since the slow dissolution of residual Na^+ from the solid takes place during the adsorption experiment. The logarithms of the K_d values increase linearly with increasing pH in the pH range studied. The selectivity sequence is $Rb^+ > K^+ > Cs^+ > Li^+$ for alkali-metal ions over the pH range studied. The selectivity sequence is different from those for other kinds of manganese oxide samples[23,24,29] ($Cs^+ > Rb^+ > K^+ > Li^+ > Na^+$ for spinel type, $K^+ > Rb^+ \gg Na^+$, $Cs^+ > Li^+$ for hollandite type, and $Cs^+ > Rb^+ > K^+ > Na^+ > Li^+$ for todorokite type). A characteristic feature is that Na-2 × 4 (H) has high selectivity for the adsorption of Rb^+ ions with an effective radius around 1.66 Å. This feature can be explained on the basis of the ion-sieve effect of the (2 × 4) tunnel sites in the Na-2 × 4 (H). A plot of log K_d against the effective ionic radius of alkali-metal

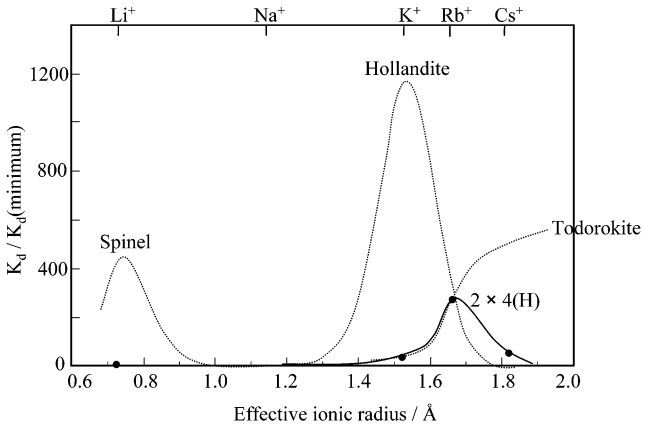

Figure 11. Distribution coefficients (K_d) of alkali-metal ions on Na-2 × 4 (H) at pH 4.0 as a function of effective ionic radius. The dotted lines are our previous results for other manganese oxides.[3]

ions[37] indicates that Na-2 × 4 (H) shows the highest K_d value around 1.7 Å (Figure 11). The result suggests that the pore size of Na-2 × 4 (H) is most suitable for fixing an ion with an effective radius of about 1.7 Å. The metal ions having the same size as adsorptive sites in the 2 × 4 tunnel structure are held strongly by Na-2 × 4 (H), while the smaller alkali-metal ions, such as Li^+ or Na^+, are loosely bound by the weaker electrostatic attraction force. On the basis of the present result, we define the radius (1.7 Å) as an effective pore radius for the ion-sieve-type adsorbent Na-2 × 4 (H).

(37) Shannon, R. D.; Prewitt, C. T. *Acta Crystallogr.* **1969**, *B25*, 925.

Conclusions

Na-2 × 4 tunnel structure manganese oxide can be prepared by hydrothermal treatment of Na−birnessite material in NaOH solution at low temperatures and low pressures. Na^+ ions in the 2 × 4 tunnel sites can be topotactically extracted from Na-2 × 4 by 10 M HNO_3 solution. Alkali-metal ions can be inserted into the 2 × 4 tunnel sites of the acid-treated sample (Na-2 × 4 (H)) by a topotactic reaction. The acid-treated sample (Na-2 × 4 (H)) shows an ion-sieve property for the adsorption of cations with an effective ionic radius of about 1.7 Å.

Acknowledgment. The authors are grateful for the financial support from the Japan Society for the Promotion of Science.

CM030344Z